simulation showed that the refolding pathway of a protein that had been mechanically stretched into a partially unfolded state involved the formation and rupture of specific hydrogen bonds (*8*). Lattice simulations have predicted that the radius of gyration (related to the end-to-end length) of a folding protein could follow a multiplicity of pathways with a time course that occurs in distinct stages (*31*). More recent simulations have predicted that after a rapid polymer collapse into a semicompact globule, the rate-limiting step for protein folding becomes the random search for any of thousands of transition states that can be reached from this semicompact form. Once a transition state is found, a rapid folding collapse ensues (*4*, *23*, *32*). This folding time course qualitatively reproduces the folding trajectories that we observed.

The direct observation of the folding trajectory of ubiquitin demonstrated here opens the way for a detailed study of protein-folding pathways. Our results contradict the generally held view that folding and unfolding reactions correspond to transitions between well-defined discrete states. In contrast, we observed that ubiquitin folding occurs through a series of continuous stages that cannot be easily represented by state diagrams. By studying how the folding trajectories respond to a variety of physical-chemical conditions (*33*), mutagenesis, and protein engineering (*34*), we may begin to identify the physical phenomena underlying each stage in these protein-folding trajectories.

References and Notes

1. U. Mayor *et al*., *Nature* **421**, 863 (2003).
2. A. Matouschek, J. T. Kellis Jr., L. Serrano, A. R. Fersht, *Nature* **340**, 122 (1989).
3. B. Schuler, E. A. Lipman, W. A. Eaton, *Nature* **419**, 743 (2002).
4. A. Sali, E. Shakhnovich, M. Karplus, *Nature* **369**, 248 (1994).
5. C. Hardin, M. P. Eastwood, M. Prentiss, Z. Luthey-Schulten, P. G. Wolynes, *J. Comput. Chem.* **23**, 138 (2002).
6. K. A. Dill, H. S. Chan, *Nature Struct. Biol.* **4**, 10 (1997).
7. C. M. Dobson, A. Sali, M. Karplus, *Angew. Chem. Int. Ed.* **37**, 868 (1998).
8. M. Gao, H. Lu, K. Schulten, *Biophys. J.* **81**, 2268 (2001).
9. E. Rhoades, E. Gussakovsky, G. Haran, *Proc. Natl. Acad. Sci. U.S.A.* **100**, 3197 (2003).
10. M. Rief, M. Gautel, F. Oesterhelt, J. M. Fernandez, H. E. Gaub, *Science* **276**, 1109 (1997).
11. M. Rief, F. Oesterhelt, B. Heymann, H. E. Gaub, *Science* **275**, 1295 (1997).
12. A. F. Oberhauser, P. K. Hansma, M. Carrion-Vazquez, J. M. Fernandez, *Proc. Natl. Acad. Sci. U.S.A.* **98**, 468 (2001).
13. Materials and methods are available as supporting material on *Science* Online.
14. S. Khorasanizadeh, I. D. Peters, H. Roder, *Nature Struct. Biol.* **3**, 193 (1996).
15. M. Carrion-Vazquez *et al*., *Nature Struct. Biol.* **10**, 738 (2003).
16. M. Carrion-Vazquez *et al*., *Proc. Natl. Acad. Sci. U.S.A.* **96**, 3694 (1999).
17. S. Vijay-Kumar, C. E. Bugg, W. J. Cook, *J. Mol. Biol.* **194**, 531 (1987).
18. The use of a greatly improved piezoelectric actuator together with soft cantilevers makes it possible to control the force and the length of a single protein with pico-Newton and nanometer resolution. However, it is still somewhat difficult to set the exact value of a low-force setting because our current force-clamp apparatus can be affected by small direct current offsets that affect our zero-force set point. These offsets do not affect our results at high stretching forces but can cause an unknown error when quenching the stretched protein to a low force. One way to independently measure the actual quenched force is to measure the magnitude of the elastic recoil that occurs immediately after relaxing the unfolded polymer chain to the lower force (e.g., steplike relaxation that coincides with downward arrows in Fig. 3). Given that in each case we know the contour length of the unfolded polypeptide, we used the wormlike chain model of polymer elasticity to find the magnitude of the force quench for each elastic recoil event.
19. P. G. de Gennes, *J. Phys. Lett. (Paris)* **46**, L639 (1985).
20. A. Y. Grosberg, S. K. Nechaev, E. I. Shakhnovich, *J. Phys. (Paris)* **49**, 2095 (1988).
21. H. Li, A. F. Oberhauser, S. B. Fowler, J. Clarke, J. M. Fernandez, *Proc. Natl. Acad. Sci. U.S.A.* **97**, 6527 (2000).
22. J. Liphardt, B. Onoa, S. B. Smith, I. J. Tinoco, C. Bustamante, *Science* **292**, 733 (2001).
23. Y. Zhou, M. Karplus, *J. Mol. Biol.* **293**, 917 (1999).
24. C. Williams, F. Brochard, H. L. Frisch, *Annu. Rev. Phys. Chem.* **32**, 433 (1981).
25. V. S. Pande, A. Y. Grosberg, T. Tanaka, *Rev. Mod. Phys.* **72**, 259 (2000).
26. A. Buguin, F. BrochardWyart, P. G. deGennes, *C. R. Acad. Sci. Paris* **322**, 741 (1996).
27. A. Halperin, P. M. Goldbart, *Phys. Rev. E* **61**, 565 (2000).
28. T. Frisch, A. Verga, *Phys. Rev. E* **65**, 041801 (2002).
29. B. Chu, Q. C. Ying, A. Y. Grosberg, *Macromolecules* **28**, 180 (1995).
30. I. Nishio, G. Swislow, S. T. Sun, T. Tanaka, *Nature* **300**, 243 (1982).
31. C. J. Camacho, D. Thirumalai, *Proc. Natl. Acad. Sci. U.S.A.* **90**, 6369 (1993).
32. Y. Zhou, M. Karplus, *Nature* **401**, 400 (1999).
33. D. K. Klimov, D. Thirumalai, *Phys. Rev. Lett.* **79**, 317 (1997).
34. S. Nauli, B. Kuhlman, D. Baker, *Nature. Struct. Biol.* **8**, 602 (2001).

35. We thank L. Li and K. Walther for helpful discussions and H. Huang for technical assistance. This work is funded by grants from NIH (J.M.F.).

Supporting Online Material

www.sciencemag.org/cgi/content/full/303/5664/1674/DC1
Materials and Methods
Figs. S1 to S4
References

14 October 2003; accepted 2 February 2004

Columnar Architecture Sculpted by GABA Circuits in Developing Cat Visual Cortex

Takao K. Hensch[1,2]* and Michael P. Stryker[2]

The mammalian visual cortex is organized into columns. Here, we examine cortical influences upon developing visual afferents in the cat by altering intrinsic γ-aminobutyric acid (GABA)–mediated inhibition with benzodiazepines. Local enhancement by agonist (diazepam) infusion did not perturb visual responsiveness, but did widen column spacing. An inverse agonist (DMCM) produced the opposite effect. Thus, intracortical inhibitory circuits shape the geometry of incoming thalamic arbors, suggesting that cortical columnar architecture depends on neuronal activity.

Columnar architecture is the hallmark of the mammalian neocortex. What determines the final dimensions of individual columns, however, remains largely unknown. Manipulations of early visual experience indicate that the segregation of eye-specific columns is a competitive process between axons serving the two eyes in primary visual cortex (*1*, *2*). Cortical target neurons detect patterns of input activity to strengthen those connections correlated with their own firing, while weakening uncorrelated afferent input. Gross disruption of postsynaptic activity supports such a correlation-based mechanism of refinement (*3*, *4*). Yet, recent reports have shown that initial clustering of individual thalamocortical arbors occurs at least a week before the critical period (*5*), leading to a suggestion that it may be largely genetically predetermined (*6*) rather than emerging from an initially overlapping configuration.

Computational models based on traditional, self-organizing principles offer specific predictions about column spacing (*7*, *8*). Local excitatory connections within cortex may spread incoming afferent activity over a certain radius, which is ultimately limited by farther-reaching inhibition. Modulating the relative balance of excitation to inhibition alters the shape of this interaction function. Activity-dependent processes acting upon narrowed or broadened central excitatory regions would ultimately

[1]Laboratory for Neuronal Circuit Development, RIKEN Brain Science Institute, 2-1 Hirosawa, Wako-shi, Saitama 351-0198, Japan. [2]W. M. Keck Foundation Center for Integrative Neuroscience, Department of Physiology, University of California–San Francisco, San Francisco, CA 94143–0444, USA.

*To whom correspondence should be addressed. E-mail: hensch@postman.riken

yield slender or wide columns, respectively (*7*, *8*). Here, we tested this hypothesis in developing kitten visual cortex.

We measured the final size of ocular dominance columns after locally altering the inhibition intrinsic to visual cortex in vivo for 1 month starting 2 weeks after birth. At this age, physiological and anatomical data show that columns are beginning to segregate (*5*). Yet, individual thalamocortical arbors in the cat extend sparse, broadly distributed processes that have yet to focus their branching (*9*). Because direct activation of γ-aminobutyric acid (GABA) receptors with muscimol disrupts column formation (*3*), we used a local enhancement of intracortical inhibition during development that does not silence cortex (Fig. 1A) (*10*).

Visual stimulation releases the endogenous inhibitory neurotransmitter GABA (*11*). Benzodiazepines are bidirectional, allosteric modulators at $GABA_A$ receptors of particular subunit stoichiometry (*12*). Agonists, such as diazepam, reversibly potentiate chloride flux through the $GABA_A$ receptor ionopore (*13*), whereas inverse agonists, such as β-carboline derivatives (methyl-6,7-dimethoxy-4-ethyl-β-carboline, DMCM), decrease $GABA_A$ currents (*14*). Benzodiazepines are inert in the absence of released GABA (*12*), making them an ideal tool to examine the endogenous role of intracortical interactions during column formation. Binding sites are highest in input layer 4 of cats at all ages but are not altered by surgical undercutting of afferents (*15*), indicating that benzodiazepine receptors are associated with intrinsic cortical elements rather than thalamocortical axons or other subcortical input.

Chronic treatment with a benzodiazepine agonist (diazepam) had little effect on the functional properties of mature cortical neurons in vivo (*10*, *16*, *17*), although inhibitory postsynaptic currents were enhanced by the drug in vitro even after 4 weeks at body temperature (37°C) (fig. S1). Optical imaging of intrinsic signals revealed robust orientation maps, and single units remained well tuned for orientation (Fig. 1, B and C). Although response strength, habituation, and spontaneous activity were not significantly affected (fig. S2), direction selectivity was consistently reduced (Fig. 1C and fig. S2). These results are typical of enhanced inhibition in computational models of cortical processing normally operating in a regime of balanced excitation and inhibition (*18*), supporting the notion that the visual cortex can recalibrate itself following alterations in neuronal activity.

However, unlike the representation in normal (*1*, *2*) or inverse agonist-treated hemispheres (Fig. 1D), a reduced binocularity appeared in the ocular dominance distribution of single units near a chronic diazepam infusion site (Fig. 1E). We then examined the overall layout of [^{3}H]proline-labeled ocular dominance columns in flattened visual cortex (*10*). Columns near the diazepam infusion site (3.5 mM; 2.5 μl/hour) were wider than columns in regions farther away or behind the cannula (Fig. 2, A and B). Such a pattern would be expected from a point source of drug flowing unidirectionally anterior to the cannula bevel (~100-fold dilution within brain tissue) (*10*, *16*). Pumping at a slower rate (0.2 μl/hour) and higher dose (35 mM) to create a larger radius of drug diffusion produced a region of unsegregated columns in front of the cannula and wide columns behind (Fig. 3B). These results reflect a continuum of GABA action approaching saturation, because potent, direct activation of $GABA_A$ receptors with muscimol desegregates columns (*3*).

In contrast to the local, graded changes in column width seen with diazepam, control hemispheres exhibited a homogeneous spacing across a similar extent of area 17

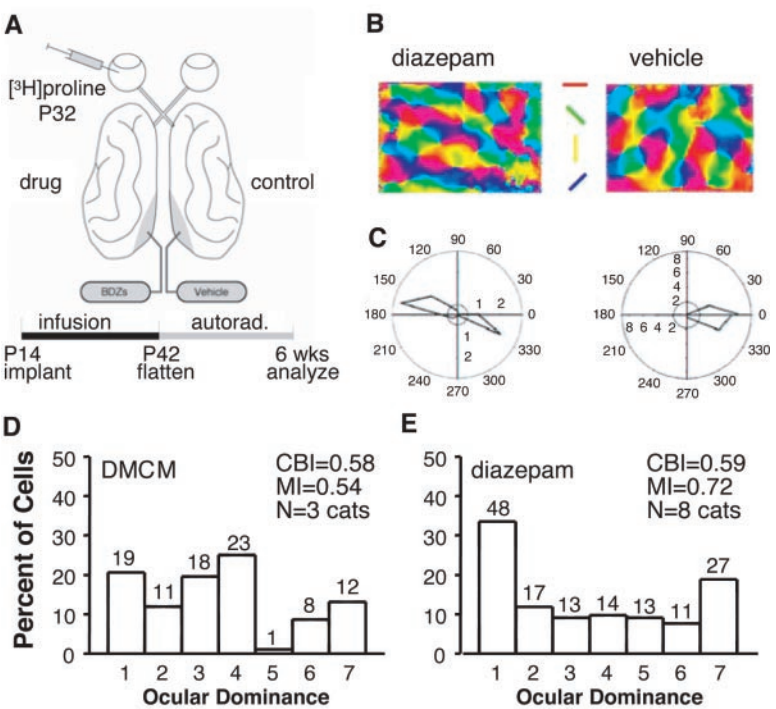

Fig. 1. (**A**) Protocol for local modulation of intrinsic inhibition in vivo. Local benzodiazepine agonist (diazepam), inverse agonist (DMCM), or vehicle (propylene glycol) was infused from osmotic minipumps (0.2 or 2.5 μl/hour) into kitten striate cortex for 4 weeks starting at 14 to 17 days after birth (*10*). Monocular [^{3}H]proline (2 mCi) was injected 10 days before electrophysiological recording. Labeled columns were measured in tangential sections through layer 4 of unfolded and flattened visual cortex (*10*). (**B** and **C**) Physiological properties of diazepam-treated cortical neurons. Robust orientation tuning in optical imaging angle maps (B) and single-unit responses (C). Spontaneous activity and response strength are indicated as respective concentric-circle radii. The absence of directionality in diazepam-treated cortex is apparent in this example (fig. S2). (**D** and **E**) Ocular dominance distribution after DMCM infusion was binocular, as in controls (D) (*1*, *2*), but diazepam-treated hemispheres were significantly less binocular (E) ($P < 0.001$, χ^2 test, DMCM versus diazepam). CBI, contralateral bias index; MI, monocularity index. The number of cells per ocular dominance group is as indicated.

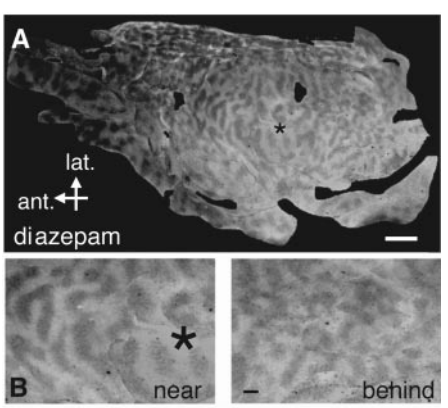

Fig. 2. (**A**) Chronic diazepam infusion widens ocular dominance columns locally. Flatmount of overall layout of labeled (dark) and unlabeled (white) ocular dominance bands in layer 4 of diazepam-infused (*) (3.5 mM, 2.5 μl/hour) kitten visual cortex. (**B**) Wide, crisp columns just anterior to the cannula site compared to an area behind and away from the infusion. Scale bars: 5 mm (A); 1 mm (B).

(Fig. 3A). To further verify the specificity of diazepam action, we successfully infused the benzodiazepine inverse agonist DMCM in three animals, but at a necessarily less than saturating dose (50 μM) to avoid the toxicity of excessive intracortical excitation. Regardless of the dose, final column spacing exhibited a trend that was the reverse from that of diazepam: Columns just in front of the cannula site were less discrete and narrower than columns farther away, behind, or in control hemispheres (Fig. 4).

We used a computer-based wavelet analysis algorithm to quantify the changes in periodicity (*19*, *20*). Interindividual variability in column spacing would obscure changes in a group comparison (*20*, *21*). We therefore expressed column widths of experimental regions as a percentage change from the mean observed in regions far from the cannula site. Column spacing across the similar extent of control hemispheres was also calculated as a fraction of the mean. We further analyzed a large control sample from the literature of flattened kitten hemispheres labeled with either 2-deoxyglucose or [^{3}H]proline (*3*, *22*, *23*). Intrinsic variability in column spacing spanned ±10 to 20% distal to a cannula site or when no drug or vehicle was infused (Fig. 5) (*20*). In contrast, the percentage increase for five of six diazepam-treated regions was greater than that in any of the controls. The remaining experimental area was near the upper extreme of the control range, whereas reducing intrinsic inhibition with subsaturating doses of inverse agonist (DMCM) consistently yielded column shrinkage toward the opposite extreme (Fig. 5).

A straightforward interpretation of our findings is that GABA-mediated inhibition controls the local competition between right and left eye inputs in visual cortex (*16*, *17*). Enhanced competition by diazepam would explain reduced binocularity of single-unit responses (Fig. 1E), as well as wider and sharper anatomical segregation near the infusion site. All three aspects are reminiscent of strabismic cats (*23*) and monkeys (*24*) in which the two eyes' inputs are maximally decorrelated (*1*, *2*). Intrinsic differences in the range of intracortical inhibition may underlie the large variability of anatomical column spacing normally found across individuals (*20*, *21*, *25*).

Not all GABA circuits may be relevant. Lateral inhibition is thought to enhance the contrast between neighboring columns in normal animals (*26*). Indeed, the model of Miller *et al*. (*7*) predicts the bidirectional changes observed here when benzodiazepines act preferentially through long range rather than local inhibition (fig. S4). Large basket cells in cat visual cortex extend a wide, horizontal axonal plexus that can span ocular dominance columns (*27*), which is useful for discriminating input coming from the two eyes. Among the great diversity of $GABA_A$ receptors (*12*), only those containing the α1 subunit drive the functional shift of ocular dominance following monocular deprivation in mice (*28*). These receptors are enriched at perisomatic synapses innervated by parvalbumin-positive large basket cells (*29*), which form coupled networks that are exquisitely sensitive for the detection and propagation of synchronized signals on a columnar scale (*30*).

Thus, our results demonstrate that inhibitory circuits intrinsic to the neocortex instruct both functional (*16*) and anatomical refinement of incoming presynaptic input (*9*) and support a self-organizing segregation process based on correlated neuronal activity (*7*, *31*) rather than a prespecified patterning of molecular cues (*6*).

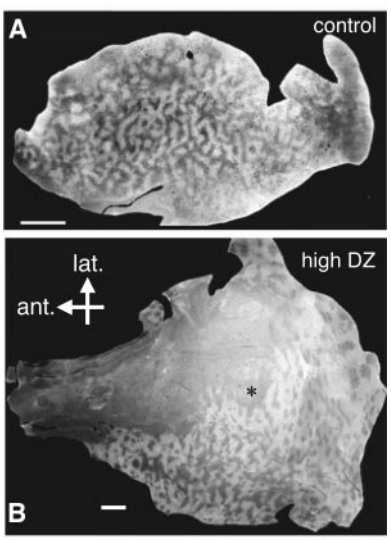

Fig. 3. (**A**) Control hemisphere exhibits relatively homogeneous column spacing across a homologous extent of area 17. (**B**) Graded effect of diazepam treatment. A high dose (35 mM, 0.2 μl/hour) yields an area of column desegregation (anterolateral to cannula site) (*) reminiscent of direct $GABA_A$ receptor activation with muscimol (*3*). Scale bar: 5 mm.

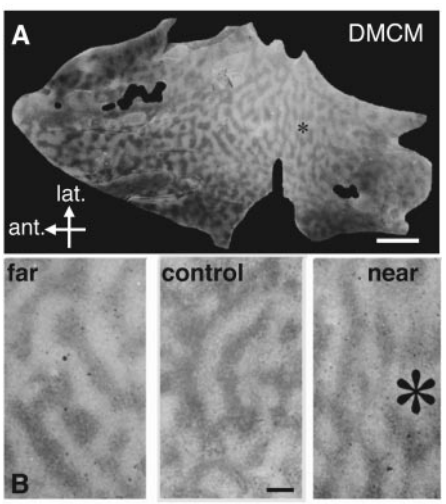

Fig. 4. (**A**) Chronic inverse agonist infusion locally reduces column size. Overall layout of labeled ocular dominance bands (dark) surrounding a DMCM infusion site (*) (50 μM, 2.5 μl/hour). (**B**) Columns near a DMCM source were blurred and narrow (right) compared to distal (left) or homologous regions in control hemispheres (middle). Scale bars, 5 mm (A); 1 mm (B).

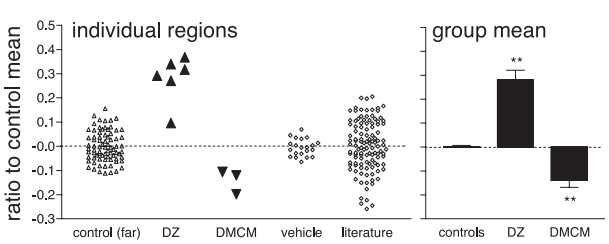

Fig. 5. Bidirectional control of developing column size by cortical inhibition. Wavelet measurements (*10*, *20*) of spacing in individual regions were normalized to control mean far from the cannula, or across vehicle and untreated control hemispheres from literature (*3*, *22*, *23*). Statistical comparison is by group. $^{**}P < 0.001$, *t* test versus control.

References and Notes

1. T. N. Wiesel, *Nature* **299**, 583 (1982).
2. N. Daw, *Visual Development* (Plenum, New York, 1995).
3. Y. Hata, M. P. Stryker, *Science* **265**, 1732 (1994).
4. Y. Hata, T. Tsumoto, M. P. Stryker, *Neuron* **22**, 375 (1999).
5. M. C. Crair, J. C. Horton, A. Antonini, M. P. Stryker, *J. Comp. Neurol.* **430**, 235 (2001).
6. J. C. Crowley, L. C. Katz, *Curr. Opin. Neurobiol.* **12**, 104 (2002).
7. K. D. Miller, J. B. Keller, M. P. Stryker, *Science* **245**, 605 (1989).
8. D. J. Willshaw, C. von der Malsburg, *Proc. R. Soc. London B* **194**, 431 (1976).
9. A. Antonini, M. P. Stryker, *J. Neurosci.* **13**, 3549 (1993).
10. Materials and methods are available as supporting material on *Science* Online.
11. T. Shirokawa, T. Ogawa, *Brain Res.* **589**, 157 (1992).
12. W. Sieghart, *Pharmacol. Rev.* **47**, 181 (1995).
13. M. Eghbali, J. P. Curmi, B. Birnir, P. W. Gage, *Nature* **388**, 71 (1997).
14. M. Capogna *et al*., *Neuropharmacology* **33**, 875 (1994).
15. C. Shaw, C. Aoki, M. Wilkinson, G. Prusky, M. Cynader, *Brain Res.* **465**, 67 (1987).
16. T. K. Hensch *et al*., *Science* **282**, 1504 (1998).
17. M. Fagiolini, T. K. Hensch, *Nature* **404**, 183 (2000).
18. D. C. Somers, S. B. Nelson, M. Sur, *J. Neurosci.* **15**, 5448 (1995).
19. M. Kaschube, F. Wolf, T. Geisel, S. Löwel, *J. Neurosci.* **22**, 7206 (2002).
20. M. Kaschube *et al*., *Eur. J. Neurosci.* **18**, 3251 (2003).

21. J. C. Horton, D. R. Hocking, *J. Neurosci.* **16**, 7228 (1996).
22. S. Löwel, W. Singer, *Exp. Brain Res.* **68**, 661 (1987).
23. S. Löwel, *J. Neurosci.* **14**, 7451 (1994).
24. A. W. Roe, G. M. Ghose, E. L. Smith, Y. M. Chino, D. Y. Tso, *Soc. Neurosci. Abstr.* **121**, 689.9 (1995).
25. D. L. Adams, J. C. Horton, *Nature Neurosci.* **6**, 113 (2003).
26. A. M. Sillito, J. A. Kemp, H. Patel, *Exp. Brain Res.* **41**, 1 (1980).
27. P. Buzas, U. T. Eysel, P. Adorjan, Z. F. Kisvarday, *J. Comp. Neurol.* **437**, 259 (2001).
28. M. Fagiolini *et al.*, *Science* **303**, 1681 (2004).
29. T. Klausberger, J. D. Roberts, P. Somogyi, *J. Neurosci.* **22**, 2513 (2002).
30. M. Galaretta, S. Hestrin, *Science* **292**, 2295 (2001).
31. D. L. Adams, J. C. Horton, *Science* **298**, 572 (2002).
32. We thank S. Harris for assistance during minipump implant surgery; J. C. Horton for advice on flat-mount histology; Y. Hata and S. Löwel for flat-mount image data of labeled ocular dominance columns; M. Kaschube and F. Wolf for the "wavelet" analysis program; and K. D. Miller and M. Fagiolini for critical comments and discussion. Supported in part by a Howard Hughes Medical Institute Predoctoral Fellowship (T.K.H.) and grants from NIH (M.P.S.).

Supporting Online Material
www.sciencemag.org/cgi/content/full/303/5664/1678/DC1
Materials and Methods
Figs. S1 to S4
References

2 September 2003; accepted 8 January 2004

Specific $GABA_A$ Circuits for Visual Cortical Plasticity

Michela Fagiolini,[1] Jean-Marc Fritschy,[2] Karin Löw,[2] Hanns Möhler,[2,3] Uwe Rudolph,[2] Takao K. Hensch[1]*

Weak inhibition within visual cortex early in life prevents experience-dependent plasticity. Loss of responsiveness to an eye deprived of vision can be initiated prematurely by enhancing γ-aminobutyric acid (GABA)–mediated transmission with benzodiazepines. Here, we use a mouse "knockin" mutation to α subunits that renders individual GABA type A ($GABA_A$) receptors insensitive to diazepam to show that a particular inhibitory network controls expression of the critical period. Only α1-containing circuits were found to drive cortical plasticity, whereas α2-enriched connections separately regulated neuronal firing. This dissociation carries implications for models of brain development and the safe design of benzodiazepines for use in infants.

Experience-dependent plasticity shapes the early postnatal brain, as exemplified by the loss of responsiveness to an eye briefly deprived of vision during a critical period, which results in severe amblyopia (poor visual acuity) (*1*). This behavioral sensitivity is reflected in the neuronal firing of single units in the primary visual cortex of mammals, including mice (*2*, *3*). Critical-period onset can be delayed indefinitely if release of the inhibitory neurotransmitter γ-aminobutyric acid (GABA) is kept low by gene-targeted disruption of the synaptic isoform of its synthetic enzyme, glutamic acid decarboxylase 65 (GAD65) (*4*). Conversely, the natural plasticity profile is accelerated by prematurely enhancing inhibition (*4*, *5*).

It remains unclear, however, whether overall inhibitory tone or a specific network controls critical-period onset. The diversity of GABA cells in the neocortex complicates local circuit analysis. Although neuronal morphology and biochemistry are heterogeneous, synaptic connections are precisely targeted (*6*). We have used the infusion of benzodiazepine agonists concurrent with monocular deprivation (MD) to prematurely trigger ocular dominance plasticity (Fig. 1A). These drugs enhance in a use-dependent manner specific GABA type A ($GABA_A$) receptor–mediated currents whose benzodiazepine sensitivity is determined by a particular α-subunit complement (*7*, *8*). This allows us to analyze here whether particular GABA circuits underlie visual cortical plasticity.

We first attempted critical-period acceleration in wild-type (C57BL/6) mice, using the subtype-selective benzodiazepine receptor agonist zolpidem (*9*). No plasticity typically occurs after a 4-day period of MD just after eye opening (Fig. 1, A and B). Instead, a strong ocular dominance shift in favor of the open eye was induced in the presence of zolpidem (Fig. 1) (χ^2 test, $P < 0.0001$ versus vehicle), as observed previously for the broad spectrum agonist diazepam (DZ) (*4*). Receptors sensitive to zolpidem include α1, α2, and α3 subunits, while the α5 subtype is less sensitive by a factor of 10,000 (*9*). The ability to shift critical-period onset with this drug at low concentration (~ 0.1 to 1 μM in cortex upon diffusion) (*10*, *11*), therefore, indicates little role for α5-containing receptors in triggering visual cortical plasticity.

Of nearly 20 identified $GABA_A$ receptor subunits (*7*), just four (α1, α2, α3, and α5), together with an obligatory γ2 subunit, contribute critical amino acid residues to the benzodiazepine binding site. Mutation of a histidine (H) to an arginine (R) renders individual GABA receptors insensitive to DZ, as occurs naturally for the α4 or α6 subtypes (*8*). Selective targeting of the homologous site in each of the α subunits produces specific impairments of the sedative, anxiolytic, and motor behavioral effects of DZ (*12*–*14*). We tested the DZ-induced critical-period acceleration paradigm in the three separate α1(H101R), α2(H101R), and α3(H126R) knockin mouse lines described previously.

Of the neocortical inhibitory interneurons, chandelier cells represent a unique example of synapse specificity, forming the fundamental source of input onto pyramidal cell axon initial segments (*6*), where $GABA_A$ receptor α2 subunits are preferentially localized (*15*–*17*). In both GAD65 knockout and pre–critical period wild-type mice, where plasticity fails to occur, single units in the primary visual cortex fire excess spikes that outlast the visual stimulus (*4*, *10*). Because axo-axonic contacts are ideally situated to regulate such a prolonged discharge phenotype, we first examined whether this particular GABA subcircuit may directly underlie visual cortical plasticity. Brief MD just after eye opening in α2(H101R) knockin mice still produced premature ocular dominance shifts when combined with DZ but not with vehicle injections (Fig. 2, A and B) (χ^2 test, $P < 0.0001$ versus vehicle).

In contrast, prolonged discharge was not corrected by benzodiazepine treatment in α2(H101R) mutant mice. The other two α3 and α1 knockin lines, as well as zolpidem treatment of wild-type mice, exhibited a normal regulation of this spiking phenotype in vivo (Fig. 2C). Thus, the disruption of neural coding in and of itself does not predict whether ocular dominance shifts will occur. Although α2-subunit-enriched (e.g., chandelier cell "cartridge") synapses may control prolonged discharge, other GABAergic connections must drive visual cortical plasticity.

We, therefore, turned our attention to α1-containing circuits. The expression of the α1 subunit in primary visual cortex is

[1]Laboratory for Neuronal Circuit Development, RIKEN Brain Science Institute, 2-1 Hirosawa, Wako-shi, Saitama, 351-0198 Japan. [2]Institute of Pharmacology and Toxicology, University of Zürich, Winterthurerstrasse 190, Zurich, CH-8057 Switzerland. [3]Department of Chemistry and Applied Biosciences, Swiss Federal Institute of Technology (ETH), Winterthurerstrasse 190, Zürich, CH-8057 Switzerland.

*To whom correspondence should be addressed. E-mail: hensch@postman.riken.go.jp